Z. Phys. B – Condensed Matter 77, 399–407 (1989)

Condensed Matter
Zeitschrift für Physik B

Thickness dependence of the work function in double-layer metallic films

H. Hornauer*, J. Vancea, G. Reiss, and H. Hoffmann
Institut für Angewandte Physik, Universität Regensburg, Federal Republic of Germany

Received May 17, 1989; revised version July 3, 1989

The work function of metallic thin films limited by symmetric surfaces is expected to be thickness dependent at a level of 0.1 eV and a thickness range of about 5 nm. Recent experiments, however, demonstrated that Cu films on glass or Ni substrates show a long ranging (10–20 nm) increase of the work function with increasing film thickness [1]. This effect was attributed to a violation of local charge neutrality in films with unlike surfaces. In this paper we show that the barrier height of thin film diodes like metal-insulator-metal (MIM)-, metal-semiconductor (Schottky contacts)- and metal-vacuum-metal (Kelvin capacitors) structures decreases with increasing thickness of one metal electrode. This metal electrode consists of a double layer whose single layer thicknesses are of the order of few tens of nm. The observed effect can be attributed to a decrease of the work function at the counter limiting interface not exposed to the evaporation beam. A possible explanation can be found again in the violation of the local charge neutrality in films with unlike surfaces.

1. Introduction

The work function at the right (r)- or lefthand (l) boundary of a thin metallic film can be expressed by:

$$\Phi(r, l)=\varphi_\infty(r, l)-E_F \tag{1}$$

where $\varphi_\infty(r, l)$ are the corresponding vacuum potentials and E_F is the Fermi level.

For symmetrically bounded films one obtains $\varphi_\infty(r)=\varphi_\infty(l)$. For this case a possible thickness dependence of the Fermi level has been intensively discussed in the literature [2–4]. Commonly the related wave vector k_F is expressed by:

$$k_F(d)=k_F(\infty)+O(1/d)+O(1/d^2) \tag{2}$$

with $O(1/d)=(1/d)(\pi/4-\langle\eta\rangle_k)$, d the film thickness and $\langle\eta\rangle_k$ the sum of the surface-induced phase shifts for the wave functions.

The assumption of local charge neutrality in the middle of a symmetric film yields the Sugiyama-Langreth phase sum rule [4] which states $\langle\eta\rangle_k=\pi/4$ and suppresses the long ranging $1/d$ term in (2).

On the other hand in [4] has been argued that an a priori assumption of local charge neutrality in the middle of a sufficiently thin film seems to be not justified.

The problem of local charge neutrality in the middle of thin films (i.e. the $O(1/d)$ term in (2) and the related thickness dependence of the work function) seems to be open for discussion.

For symmetric thin films Schulte [2] calculated the work function within a self consistent Lang-Kohn scheme. He obtained a thickness dependence of Φ up to $d\simeq 5$ nm, scaling with $1/d^2$. This is much larger than the classical screening length and can be attributed to the existence of the long ranging Friedel oscillations related to the limiting boundaries.

For unsymmetrically bounded and sufficiently thin films it seems to be even more suspicious to assume the existence of a bulk like region in the middle of the film. A more pronounced thickness dependence of Φ therefore can be expected.

Real thin films usually are supported by a substrate, i.e. they are limited by two distinct and different

* *Present address:* Gesamthochschule Kassel, D-3500 Kassel, FRG

interfaces. Experimentally available films therefore always correspond to unsymmetric systems. Additional unsymmetry can be produced by unsymmetric potential wells due to an adsorbate layer at one film interface or by a double layer metallic film with different charge densities.

The problem of films with unsymmetric surfaces seems to be not yet understood both from theoretical and experimental point of view.

Recently a long ranging $(1/d)$ dependence of the work function at the *film-vacuum interface* (exposed to the evaporation beam) of Cu films on Corning glass was described in [1].

The increase of the work function with increasing film thickness was at a level of 0.1–0.2 eV according to the theoretical expectations. This effect was discussed in terms of a violation of local charge neutrality in films with unlike surfaces.

Moreover a clear increase of the work function with increasing film thickness was observed for Cu films supported by 100 nm thick Ni films [1]. These films, however, show a thickness dependent work function only in the presence of an adsorbate layer at the Cu-Ni interface, i.e. for a highly unsymmetric thin film system.

In contrast with [1] this paper deals with the work function at the *counter limiting boundary* (not exposed to the evaporation beam) of *double layered films* with an adsorbate separation layer between the stacked metal layers.

The thickness of the metallic support (basic layer), however, now was varied between 8 and 60 nm. In this case the limiting boundaries of the double layer may start to interact.

This system now is more complicated than the single layer case: If the (highly unsymmetric) coating layer shows a long ranging thickness dependent work function, a $(1/d)$ violation of the local charge neutrality for this part of the double layer can be suspected. This, however, will cause thickness dependent matching conditions at the separation between basic and coating layer. In turn, even at the counter boundary of the basic layer, a corresponding long ranging thickness dependence of the work function can be expected as long as the thickness of this basic layer does not exceed the range of the charge density perturbations.

In this paper systematic investigations of the thickness dependent work function at this limiting boundary (not exposed to the evaporation beam) of a double layer metallic film are discussed. The experiments were performed with measurements of the barrier height to a massive electrode (reference electrode) using metal-insulator-metal (MIM) diodes, Schottky contacts and vibrating capacitors as "work function detectors".

2. Experimental results

As already mentioned, the aim of the experiments is the measurement of the work function of a double layer at the external boundary of the basic layer as a function of the increasing thickness of the coating layer.

For this purpose the barrier height between the basic layer and a reference electrode was measured as a function of the thickness of the coating layer in three independent experiments.

The main advantage of this approach is clear: If trivial (interfacial) effects can be excluded, any effects in the work function at the counter boundary, not exposed to the evaporation beam, of a double layer will be only due to the increasing thickness (d) of the cover layer. Effects arising from structural changes of the film surface during the film growth are therefore excluded.

A. Metal-Insulator-Metal (MIM) diodes

In the simple case of a trapezoidal potential barrier (not biased) [5], the barrier height $(\bar{\Phi})$ between the reference electrode (1) and the basic layer (2) (see Fig. 1a and b) is given by:

$$\bar{\Phi} \approx (1/2)\{\Phi_1(=\text{const.}) + \Phi_2(d)\} - \Phi_{im}(\text{const.}) \qquad (3\text{a})$$

with

- Φ_1 – the work function of the reference electrode which is expected to be constant,
- $\Phi_2(d)$ – the work function of the double layer at the basic layer-insulator interface and
- Φ_{im} – the correction due to image forces.

The tunnelling conductivity is expressed by the following complex relation [6]:

$$G(U) = (\mathrm{d}/\mathrm{d}U)\left((2e/\hbar)\int_0^\infty \mathrm{d}E \cdot \xi_1(E)\,\xi_2(E+eU) \cdot (f(E) - f(E+eU))\int_0^E \mathrm{d}E_\perp \cdot T(E_\perp, E, U)\right) \qquad (3\text{b})$$

where E is the energy, U the bias voltage, f the Fermi distribution, ξ_1, ξ_2 the densities of states in the two electrodes and T the transmission of the potential barrier ($\perp$ denotes the direction normal to the tunnelling barrier).

For an idealized trapezoidal potential barrier the WKB-approximation yields [7]:

$$T \simeq \exp(-(2D/\hbar)\cdot(2m\bar{\Phi})^{1/2})) \qquad (3c)$$

with D the thickness of the tunnelling barrier and $\bar{\Phi}$ given by (3a).

a) Experimental details

The tunnelling conductivity of Al-Al_2O_3-Me (Me = Al, Cu, Ag, Ni) diodes was investigated during the evaporation of the Me-electrode on the previously prepared Al-Al_2O_3 sandwiches. The MIM-diodes used in our experiment are sketched in Fig. 1a.

The experiment procedeed in three steps:
i) Firstly 200 nm thick Al films were evaporated on cleaned Corning glas substrates at 420 K. Subsequently the films were exposed to 10^{-2} mbar of oxygen for two hours at 360 K; insulating Al_2O_3 overlayers were obtained showing electrical resistivities between 10^3 to 10^6 Ω/mm^2.
ii) In the second step the Al-Al_2O_3 sandwiches were transferred to UHV (base pressure 10^{-9} mbar) and subsequently covered with a basic metallic layer in order to form a tunnelling diode. The tunnelling conductivity at zero bias voltage was measured during the evaporation as a function of the film thickness (lock-in technique). The film thickness was monitored by a quartz oscillator balance with a relative accuracy of 0.1% [8].

Due to the coalescence of the basic layer, the onset of the tunnelling current was at a critical thickness of about 2 nm. The following steep increase of the tunnelling conductivity up to a thickness of 4 nm was due to the further development to a compact film. In order to form a double layer metal electrode, we stopped the deposition of the basic layer at certain thicknesses (larger than 8 nm) and annealed the MIM diode for 24 h at 300 K in 10^{-9} mbar. We thereupon get a stable tunnel diode whose conductivity did no more change in time; during annealing the surface of the basic layer was contaminated with residual gas adsorbates.

Only the well known parabolic dependence of the tunnelling conductivity on the bias voltage ($G(U)$) [9] was observed for the MIM-diodes described above. Additionally these diodes show only a weak $G(\Theta^2)$ (Θ = the temperature) dependence. The characteristics mentioned above ($G(U)$, $G(\Theta^2)$) correspond to typical Al_2O_3 junctions with $\bar{\Phi} \simeq (1\text{–}1.5)$ eV and $D \approx 3$ nm [10].
iii) In the third step, which represents the central point of the experiment, this basic layer (see Fig. 1a) was covered with the same metal or an other of the four metals given before. The tunnelling conductivity was monitored as a function of the additional thickness Δd of the coating layer. The principle of the experiment is sketched in Fig. 1b.

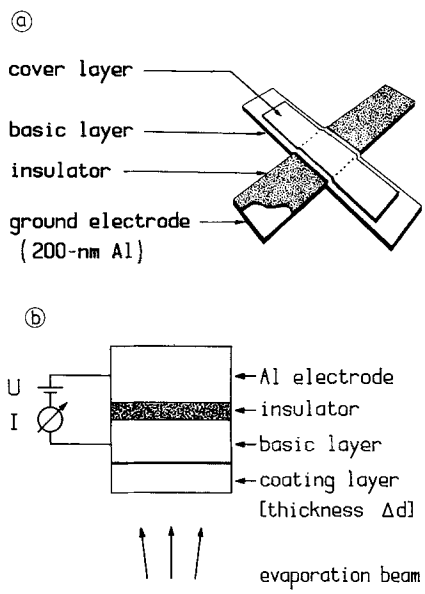

Fig. 1a and b. Experiments with MIM diodes: **a** The construction of the MIM diodes used for the observation of the thickness dependent tunnelling conductivity. **b** The principle of the experiment

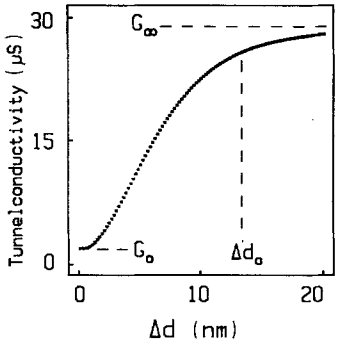

Fig. 2. The tunnelling conductivity of a MIM diode with a 18 nm thick Cu basic layer (see Fig. 1) vs the additional thickness Δd of a Cu coating layer

b) Results

The dependence of the tunnelling conductivity $G(\Delta d)$ on the additional thickness Δd is shown in Fig. 2 for a 18 nm thick Cu basic layer coated with Cu: an increase of the tunnelling conductivity by a factor 15 can be observed.

For all combinations of basic and coating layers, similar thickness dependences (Fig. 2) have been observed, with the 0.9 fraction of the asymptotic value

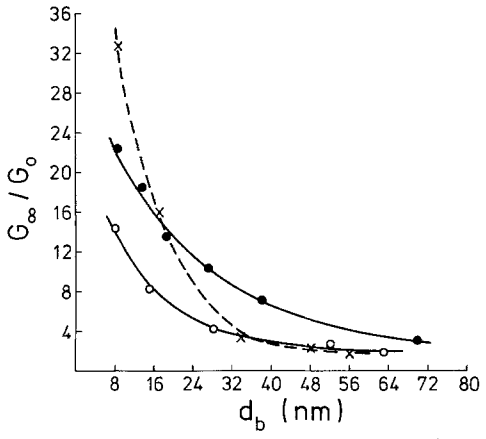

Fig. 3. Relative changes of the tunnelling conductivity vs thickness of the basic layer. ●●● Cu-basic layers condensed at 300 K, $\rho \simeq 7$ μΩcm; ○○○ Cu-basic layers condensed at 77 K, $\rho \simeq 13$ μΩcm; × × × Ni-basic layers condensed at 77 K, $\rho \simeq 29$ μΩcm

G_∞ at a characteristic thickness Δd_0. The ratio $R = G_\infty/G_0$ was typically between 10 and 30 at Δd_0 between 2 and 20 nm. In the covered state both the parabolic and the weak Θ^2 dependence of the tunnelling characteristics were maintained; therefore changes of the tunnelling mechanism itself can be excluded. Systematic results will be outlined in the following; the examples given below relate to MIM-diodes of comparable quality.

Dependence of R on the thickness of the basic layer. Cu or Ni basic layers of various thickness were evaporated in order to obtain stable tunnelling diodes in the manner described above (steps i) and ii)). Regardless their condensation temperature, the subsequent annealing procedure at 300 K (see step ii)) was carried out in all cases in the same way.

Figure 3 shows $R = G_\infty/G_0$ as a function of the basic layer thickness (d_b) for Cu-coating layers condensed at 77 K. Note that, owing to the low condensation temperature, diffusion processes are very improbable.

In all cases a clear decrease of $R = G_\infty/G_0$ with increasing thickness of the basic layer can be observed. The differences between the three curves are clearly correlated with the different resistivities of the basic layers (see Fig. 3). These resistivities are produced by different scattering mechanisms (at surfaces, at phonons, at defects and at grain boundaries) of the conduction electrons. For details see [8, 11, 12].

The influence of the coating layer. A similar behaviour can be found for different coating layers. Note that our experiment monitored in fact the dependence of the tunnelling conductivity on the thickness of this layer. Three typical results are given in Table 1.

Table 1. The value of $R = G_\infty/G_0$ and Δd_0 (see Fig. 2) for different coating layers (the condensation temperature is given in pharanthesis). The 19 nm thick Cu-basic layers were condensed at 300 K; ρ represents the resistivity of the coating-layers

Coating layer	ρ (μΩcm)	Δd_0 (nm)	G_∞/G_0
Cu (300 K)	19	18.5	12.9
Cu (77 K)	54	10.2	9.8
Ni (300 K)	35	4.4	17.1

This time basic layers of constant thickness (19 nm) and evaporation conditions (condensation temperature 300 K) with a resistivity of about 10 μΩcm have been selected.

The condensation temperature of the coating layers (in parenthesis) together with the estimated resistivities of these layers are also given in Table 1.

Again the characteristic thickness Δd_0 correlates with the resistivity of – in this case – the coating layer.

Exclusion of trivial effects. Three possible mechanisms which could produce interfacial effects and consequently changes in the tunnelling conductivity will be discussed:

Mechanical stress: The appearance of mechanical stresses during the evaporation of the coating layers could produce changes at the metal-insulator (Al_2O_3) interface. This effect, however, would be effective for insulating and semiconducting coating layers, too.

An increase of the tunnelling conductivity, however, was observed only in the case of metal- but not of insulating (SiO_2) or semiconducting (Si)-coating layers. Mechanical stress therefore does not seem to be responsible for the observed increase of the tunnelling conductivity.

Diffusion: Diffusion of metal or adsorbate atoms through the basic layer could be responsible for an enhanced tunnelling conductivity, too.

Firstly a diffusion effect of metal atoms from the coating layer to the insulator through the basic layer usually would produce an appreciable increase in the resistivity of the basic layer. Consequently the resistivity of the double layer monitored during the evaporation would permanently increase with increasing thickness of the coating layer. This has not been observed during our experiments. Secondly diffusion effects are usually strongly time dependent. Experimental observations, however, exclude diffusion effects: The evaporation of the coating layer was interrupted at a value of Δd where $R = G_\infty/G_0$ reached only half its asymptotic value; the time dependence of the tunnelling conductivity was subsequently monitored. For one hour only a constant value was observed. Effects induced by diffusion can be therefore excluded.

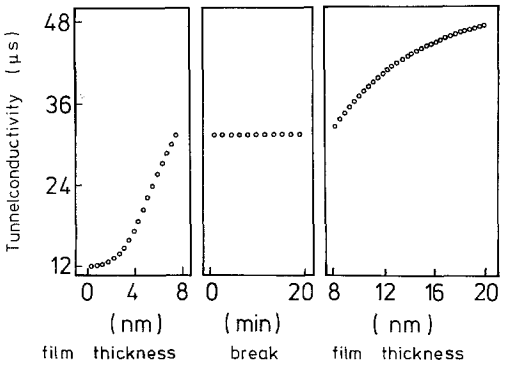

Fig. 4. Thickness dependent tunnelling conductivity of a MIM-diode (with a break of 20 min during the evaporation of the coating layer at 77 K) vs the additional thickness of a Cu coating layer. The Cu-basis layer (25 nm thick) was evaporated at 77 K

Voids in the basic layer: This would be the most trivial effect explaining an increase of the tunnelling conductivity. The following experimental observation disprove this eventuality: Cu-basic layers have been covered with Cu-coating layers up to the ranges of Δd where asymptotic (final) values are observed. Now all supposed voids should be closed. Nevertheless a subsequent coverage with Ni produced a new typical G_∞/G_0 vs Δd dependence.

c) Discussion (NIM)

In summary the result shown in Fig. 4 demonstrates that the observed increase of the tunnelling conductivity represents an authentic size effect. The evaporation of the Cu coating layer (on a Cu basic layer kept at 77 K) was interrupted for 20 min and subsequently continued. During the break the value of the tunnelling conductivity remains unchanged. Ultimately a simple parallel translation is necessary to fit perfectly the curves given in Fig. 4 to a typical thickness dependence (Fig. 2).

Consequently the observed size effect of the tunnelling conductivity has to be explained by an analysis of the different terms of (3).

Since the aluminium electrode (1) and the insulator (Al_2O_3) remain unchanged in this experiment (see Fig. 1a, b), the reason should be located in the second electrode (double layer) of the MIM structure. Variations in the density of states by a factor 30 are unphysical for clean metals. Therefore the strong increase in the tunnelling conductivity can be produced only by a thickness dependent barrier transmission (T) (Eq. (3c)). This can be due only to a variation of the work function Φ_2 of the double-layer at the Al_2O_3-basic layer interface.

For small values of $\Delta\bar{\Phi}/\bar{\Phi}$, Eqs. (3b) and (3c) lead to:

$$G_\infty/G_0 \simeq \exp((D/\hbar)\cdot(2m\bar{\Phi})^{1/2}\cdot(\Delta\bar{\Phi}/\bar{\Phi})). \quad (4)$$

Using (3a) and typical values of $G_\infty/G_0 \simeq 20$, $\bar{\Phi} \simeq$ (1–1.5) eV and $D \simeq 3$ nm a value of $\Delta\bar{\Phi}_1 \simeq 2\cdot\Delta\bar{\Phi} \approx$(0.3–0.4) eV, can be estimated.

This value depends on the thickness of the basic layer and corresponds to the values observed at the counter limiting filmvacuum interface (exposed to the evaporation beam) for the case of films with unlike surfaces [1].

The thickness range is larger than expected for symmetric thin films, i.e. this size effect should not occur for symmetrically bounded films. A size effect was observed only in the presence of an adsorbate layer between the stacked single metallic layers; this was also a precondition for the occurrence of a thickness dependent work function of the same thickness range at the other limiting surface (coating layer-vacuum interface) of a double layer [1].

Nevertheless a new problem appears: At the interface basic layer-insulator the work function decreases with increasing film thickness in contrast with the observed increase at the coating layer-vacuum interface [1].

B. The thickness dependence of the contact potential difference (Kelvin method)

The vibrating capacitor method (Kelvin method [13]) provides a simple but very sensitive detection of relative changes in the work function of a conducting surface. The principle is sketched in Fig. 5a. The reference electrode vibrates in front of the thin film surface whose work function should be determined.

The contact potential difference CPD between sample and reference (see Fig. 5a) is expressed by:

$$\mathrm{CPD} = \Phi(d) - \Phi_{\mathrm{ref}} \quad (5)$$

where $\Phi(d)$ is the work function of the double layer at the boundary not exposed to the evaporation beam. The metallic support (basic layer) consists of a 20 nm thick Au film (deposited at 500 K in 10^{-9} mbar) covered with a 5 nm Cu film. The NaCl substrate was removed after evaporation (dissolved in distilled water). Copper was used in order to fill eventually existing voids of the Au-film. The thickness of the basic layer therefore is within the range of thickness dependent work functions for comparable MIM-diodes.

The resulting free films were controlled for ruptures and voids by electron microscopy. Only films free of such defects were used for the CPD-measurements (see Fig. 5a and b).

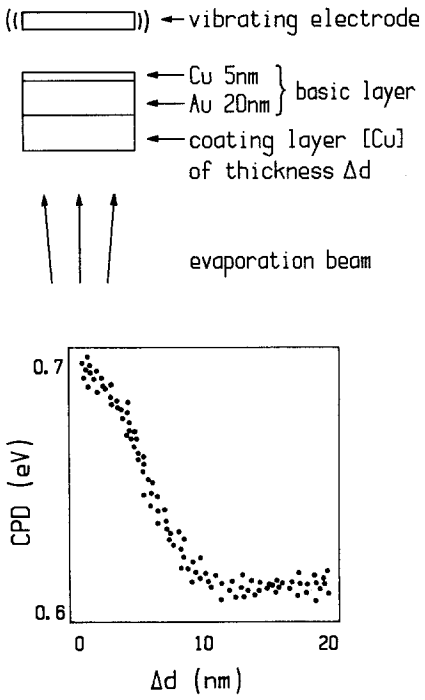

Fig. 5a and b. The measurement of the thickness dependent contact potential difference (CPD) with the Kelvin method: **a** The principle of the experiment; **b** The dependence of CPD on the additional thickness Δd of a Cu coating layer

These basic layers then were placed with the Au surface on fine meshed Cu-grids and covered in UHV through the Cu mesh with an additional Cu film of thickness Δd (coating layer). The (vibrating) reference electrode was located to the Cu limiting surface of the basic layer not exposed to the evaporation beam (Fig. 5a). Great efforts have been made in eliminating error sources arising from trivial effects as diffusion, voids, etc. [14]. The observed dependence of the CPD (see Eq. (5)) on the thickness of the coating layer for the situation sketched in Fig. 5a is shown in Fig. 5b. This clearly confirms the main result of the foregoing tunnelling experiments: At the external boundary (not exposed to the evaporation beam) of the basic layer, an evident decrease of the work function with increasing thickness of a coating layer can be observed. This effect again is of long thickness range. The relative change of the work function is at a level of 0.1 eV, i.e. of the same order of magnitude as obtained from tunnelling experiments; one notices, that in this experiment the thickness of the basic layer amounts to 25 nm.

C. *Schottky contacts*

The transmission of electrons through Schottky barriers is influenced by the metal's work function.

The Schottky barrier height (V_{MS}) is roughly expressed by:

$$V_{MS} = \Phi_m(d) - \chi - \Delta \tag{6}$$

with

$\Phi_m(d)$ – the work function of the metallic electrode (double layer) at the MS-interface,
χ – the electron affinity of the semiconductor,
Δ – the interfacial dipole due to the semiconductor surface states (dangling bonds).

Following the original theory of Schottky [15], the height V_{MS} of the Schottky barrier depends only on the difference of the work function of the metal (Φm) to the electron affinity of the semiconductor (χ), i.e. will be given by (6) for $\Delta = 0$.

As shown by Bardeen [16] this ideal barrier height (Schottky limit) is reduced owing to the existence of semiconductor surface states ($\Delta \neq 0$). In the "Bardeen limit" the density of surface states at the semiconductor surface is very large, i.e. the Schottky barrier height becomes independent of the metal work function.

Additionally, for conventionally manufactured Schottky contacts, a native oxide barrier in the order of 1–2 nm gives rise to a separation layer between the metal and the semiconductor. This separation layer will be mainly produced during the exposure to the ambient pressure. Adsorbed layers reduce the density of the surface states by completing the broken covalent bonds [17].

The following empirical rule of thumb concerning the dependence of the Schottky barrier height on the metal work function was derived from a vaste collection of experimental data [18]:

$$V_{MS} \simeq c_1 \cdot \Phi_M + c_2 \quad \text{(eV)}. \tag{7}$$

The coefficients in (7) are characteristics of the semiconductor, depending on the density of surface states which varies from experiment to experiment; the quantitative meaning of this equation therefore should not be overestimated.

Limiting values of c_1 and c_2 for various n-type semiconductors have been obtained by Sharma and Gupta [19] from experimentally available data. For n-Si they obtained:

$$0.11 \leqq c_1 \leqq 0.19 \quad \text{and} \quad -0.34 \leqq c_2 \leqq 0.35.$$

With respect to the thickness dependence of the work function of a metal film an additional effect can be expected: The Schottky barrier height should depend on the thickness of the metal electrode.

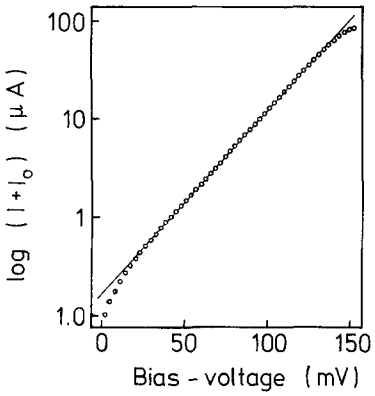

Fig. 6. The current voltage characteristic of a Cu–*n*-Si Schottky contact with a 25 Cu-basic metal electrode ($\Theta = 250$ K). The straight line was fitted conforming to (8)

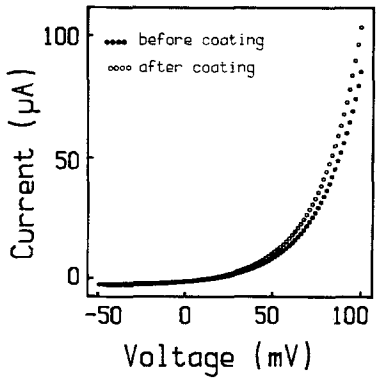

Fig. 7. The effect of a double layer metal electrode on the current-voltage characteristics of a Cu–*n*-Si Schottky contact ($\Theta = 250$ K): ●●● for a 25 nm thick Cu basic metal electrode; ○○○ after coating with a 25 nm thick Cu film

Experimental details. Cu–(*n*-Si) Schottky contacts have been used for this experiment. The semiconductor was a (100)-Si wafer ($\rho \approx 3.7$–6.25 Ωcm) covered with 3 μm thermally grown oxide. The contact geometry on the wafer was realized by common chemical etching (HF) followed by heating at 1100 K.

The wafers were subsequently mounted in an UHV evaporation system and annealed at 550 K for some days.

Thereafter a first (basic layer) 25 nm thick Cu film was evaporated in 10^{-9} mbar at a substrate temperature of 400 K. The obtained Schottky contacts are of standard quality. A typical current-voltage characteristic at $\Theta = 250$ K is given in Fig. 6, showing an exponential behaviour according to [20]:

$$I(U, \Theta) + I_0(\Theta) = I_0(\Theta) \cdot \exp(qU/nk\Theta) \tag{8}$$

with

$$I_0(\Theta) = A\Theta^2 \cdot \exp(-qV_{MS}/k\Theta) \tag{8a}$$

and A – the effective Richardson constant.

The value of I_0 in Fig. 6 was obtained by computer fitting. The parameter n of (8) represents the "ideality factor" given by the slope of the straight line in Fig. 6; for $n = 1$ the Schottky contact will be in the Bardeen limit. Values of $n > 1$ are typical for Schottky barriers with interfacial native oxide. For Cu on Si(100) we obtained n values varying between 1.05 and 1.8.

The barrier height value of (0.8 ± 0.1) eV was obtained from measurements of the temperature dependence of $(dI/dU)_{U=0}$ for 220 K $< \Theta <$ 300 K.

Results. The subsequent experimental procedure was analogous with the foregoing experiments (A and B), i.e. the basic layers were annealed in 10^{-9} mbar at 300 K for one day and then covered again with 25 nm Cu films. The current-voltage characteristic can hardly be monitored during the evaporation due to the photocurrents caused by the evaporation source. We therefore compared the current-voltage characteristics before and after evaporation. Figure 7 shows the example of a Schottky contact with $n = 1.2$. The double layer electrode gives rise to a characteristic with an emission current enhanced by about 20%. The substrate temperature (250 K) was kept constant ($\Delta\Theta < 0.1$ K) during these measurements. Due to the low heating power (150 watts) of the evaporation source and its relatively large separation to the substrate (40 cm) mounted on a massive cooled Cu-block, the heating of the sample during the evaporation was smaller than 0.4 K. Nevertheless, in order to exclude eventual temperature effects, we additionally monitored the Schottky-characteristics before and after the evaporation for several times.

The ohmic resistance of the Schottky contact (this term was neglected in (8)) is diminished ($\Delta R_\Omega \simeq 2\ \Omega$) due to the increased thickness of the metal electrode. It can be simply evaluated that this effect leads only to a minor enhancement of the current ($\Delta I/I \simeq 2 \cdot 10^{-4}$).

Finally the observed enhancement of the Schottky current can be attributed to a drop of the barrier height V_{MS}. The change of the Schottky barrier height was calculated directly from the current-voltage characteristics recorded before and after the evaporation of the coating layer using the relation:

$$\Delta V_{MS} = (k\Theta/q) \cdot \ln(I_1/I_2)_{U=\text{const}}. \tag{9}$$

For the example presented in Fig. 7, $\Delta V_{MS} = 4$ meV has been obtained.

It should be mentioned, however, that only barriers having an insulating interface at the contact region ($n \geqq 1.2$) showed the effect discussed above. This allways was at a level of (4–5) meV. For barriers with ideality n close to one, no significant effect was observed. The reason seems to be clear: only a reduced density of the semiconductor surface states due to the native oxide layer allows a dependence of the Schottky barrier height on the metal work function.

Roughly the same situation as in the foregoing experiments (A and B) can be assumed, except that the "work function detector" now is realized by a Schottky-contact. This, however, is not as sensitive to variations of the work function of the metal electrode as the foregoing methods since:

$$\Delta V_{MS}^{*} = (0.11\text{–}0.19) \cdot \Delta \Phi_m \quad \text{(see Eq. (7))}.$$

Assuming a change of the metal work function $\Delta \Phi_m$ at the contact interface of about 0.1 eV (compatible with the foregoing experiments) $\Delta V_{MS}^{*} \approx (10\text{–}20)$ meV results. Therefore, despite the somewhat rough approximations, reasonable agreement with the foregoing results was obtained.

The main result of this experiment should be noted: Despite of the different conduction mechanisms, again a decrease of the potential barrier has been observed. This result agrees with the main result of the foregoing experiments: At the external boundary (not exposed to the evaporation beam) of a basic metallic layer, the work function decreases due to the increasing thickness of a metallic coating layer.

Finally all the experiments presented above show good qualitative consistency: sign and thickness range of this effect remained unchanged regardless of different experimental circumstances.

3. Discussion

In this work we investigated the thickness dependence of the work function at the boundary of a metallic double layer opposite to the metal-vacuum interface and the evaporation beam.

One surface of a thin metallic layer (basic layer) formed a diode-configuration (MIM, vibrating capacitor, Schottky contact) with a massive electrode (reference). The other surface of this layer was exposed to the evaporation beam in order to form a double layer.

Therefore these double layers posses three different interfaces:

– an *external metal-vacuum interface*, i.e. the coating layer-vacuum interface exposed to the evaporation beam,

– an *external metal-substrate interface*, i.e. the basic layer-barrier (diode) interface not exposed to the evaporation beam, and

– an *internal metal-metal interface*, i.e. the interface between the stacked layers of the double layer.

A decrease of the barrier height with increasing thickness of the coating layer has been observed. The barrier height, however, is influenced by the work function of the double layer at the metal-substrate interface. The reduction of the barrier height can therefore be explained by a corresponding long ranging decrease of the work function at the metal-substrate interface of the double layer.

Three important results concering this new effect should be noted:

a) A decrease of the work function at the metal-substrate interface could be observed only in the presence of an adsorbate layer between the stacked metallic layers.

b) The range of this effect scales with the resistivities of the metallic films involved.

c) Whereas at the metal-vacuum interface the work function increases with increasing film thickness [1], just the opposite, i.e. a decreasing Φ has been observed at the metal-substrate interface.

Concerning point *a)* this can be attributed to a much higher degree of unsymmetry owing to the adsorbate layer. Whereas in absence of this adsorbate the electron densities only shows a crossover between the comparable values of the two metals (Cu/Cu or Cu/Ni), an adsorbate layer causes a steep decrease of the electron density at the metal-metal interface.

Therefore – following the discussion in the introduction – a long ranging thickness dependence of Φ is most probably in the presence of an adsorbate layer at the metal-metal interface.

Point *b)* seems to cause serious problems: Whereas the theoretical considerations (following [4] for example) yield an upper limit for the range of the thickness dependent work function of about 30–40 nm, no direct connection with electrical resistivities seem to exist. On the other hand nearly all calculations of Φ pretend electron states extending from one boundary to the other. This, however, can be assumed only as long as the film thickness does not exceed the characteristic length for phase destroying electron scattering (l^*).

The thickness range will therefore be limited either by the value of 30–40 nm discussed above or – in case l^* is shorter than this – by l^*. The correlation with the film resistivities could therefore be understood as a result of incoherent scattering of electrons.

The reversed sign of the thickness dependent variation of the work function (point *c)*) at the two opposite surfaces of a double layer is not yet understood.

Unsymmetric potentials, however, give rise to an additional dipole which has to be compensated in order to maintain the global electric field neutrality. This dipole can be compensated by a static transfer of charges accross the film thickness. Owing to the fact that only dipole charges are involved, the reversed sign at the two opposite surfaces can be suspected to be a consequence of this mechanism.

In summary, a thickness dependent work function at the metal-substrate interface of double-layer metallic films has been observed in three independent experiments. This long ranging effect is attributed to a strong violation of the local charge neutrality in the middle of each layer owing to the highly unsymmetric charge density profile of the whole arrangement. In agreement with the values found for single layers [1], this effect can be observed only as long as the thicknesses of the stacked metallic layers do not exceed the limiting values discussed above.

This discussion, however, offers only a qualitative explanation of these new effects. Efforts concerning the theoretical description of the observed thickness dependent work functions in films with unsymmetric surfaces are in progress [21].

References

1. Vancea, J., Reiss, G., Butz, D., Hoffmann, H.: Europhys. Lett. **9**, 379 (1989)
2. Schulte, F.K.: Surf. Sci. **55**, 427 (1976)
3. Appelbaum, J.A., Blount, E.I.: Phys. Rev. B **8**, 483 (1973)
4. Rogers III, J.P., Feuchtwang, T.E., Cutler, P.H.: Phys. Rev. B **34**, 4346 (1986)
5. Simmons, J.G.: J. Appl. Phys. **34**, 328 (1963)
6. Burnstein, E., Lundquist, S.: Tunnelling phenomena in solids, pp. 33. New York: Plenum Press 1969
7. Harrisson, W.A.: Phys. Rev. **123**, 85 (1961)
8. Vancea, J., Hoffmann, H., Kastner, K.: Thin Solid Films **121**, 201 (1984)
9. Brinkmann, W.F., Dynes, R.C., Rowell, J.M.: J. Appl. Phys. **41**, 1915 (1970)
10. Hornauer, H.: Dissertation, University of Regensburg 1987
11. Vancea, J., Reiss, G., Hoffmann, H.: Phys. Rev. B **35**, 6435 (1987)
12. Reiss, G., Vancea, J., Hoffmann, H.: Phys. Rev. Lett. **56**, 2100 (1986)
13. Lord Kelvin: Philos. Mag. **46**, 82 (1898)
14. Hornauer, H., Vancea, J., Hoffmann, H.: (submitted for publication)
15. Schottky, W.: Naturwiss. Z. **26**, 843 (1938)
16. Bardeen, J.: Phys. Rev. **71**, 717 (1947)
17. Cowley, A.M., Sze, S.M.: J. Appl. Phys. **36**, 3212 (1965)
18. Sze, S.M.: Physics of semiconductor devices, p. 376. New York: John Wiley 1969
19. Sharma, B.L. (ed.): Metal semiconductor Schottky barrier junctions and their application, p. 143. New York: Plenum Press
20. Crowell, C.R., Sze, S.M.: Solid State Electron. **9**, 1035 (1966)
21. Reiss, G.: Dissertation, University of Regensburg 1989

J. Vancea, G. Reiss, H. Hoffmann
Institut für Angewandte Physik
Universität Regensburg
Universitätsstrasse 31
D-8400 Regensburg
Federal Republic of Germany

H. Hornauer
Gesamthochschule Kassel
D-3500 Kassel
Federal Republic of Germany